Constrained Predictive Control Of A Servo-Driven Tracking Turret

P. Martin* N. Brignall M. MacDonald** M.J. Grimble*****

**Ricardo, Control and Electronics Department, Shoreham-by-Sea, England, UK*
(e-mail: peter.martin@ricardo.com)
***Selex Sensors & Airborne Systems, Avionics Division, Edinburgh, Scotland,UK*
**** Industrial Control Centre, University of Strathclyde, Glasgow, Scotland,UK*
(e-mail: m.grimble@eee.strath.ac.uk)

Abstract: Vehicle-mounted 2-axis turrets are widely used in high bandwidth tracking systems, frequently encountered in air-to-ground, ground-to-air and air-to-air targeting. Existing controllers for these systems are generally implemented in classical proportional-integral-derivative (PID) form. The objective of this paper is to examine the novel application of constrained model predictive control (MPC) to a Selex turret simulation. The characteristics of the control problem are well matched to MPC, as hard saturation constraints are present in the electrical subsystem and a reference trajectory can be generated for several seconds in advance due to the predictability of a missile trajectory. The state-space model and Kalman filter are described, and simulation results are presented to demonstrate the validity and superior performance of the MPC method.

1. INTRODUCTION

Electromechanical systems for tracking from a moving platform are widely used in defence applications for target following on board ships, aircraft or ground vehicles. The targeting system in this paper consists of three main bodies: an aircraft, the turret azimuth body or 'forks', and the turret elevation body or 'drum'. The forks and drum constitute the 'outer axes' gimbals, which are orthogonal and enable coarse target following.

The two main bodies, turret azimuth and elevation, are described by differential equations relating input and disturbance torques and friction to output angular acceleration and rate, as in Masten (1996). The aircraft and forks are linked by a geared motor that rotates the forks about the azimuth axis. The forks and drum are then linked by a geared motor that rotates the drum about the elevation axis. The geared motors and pulse width modulated (PWM) supply are described by direct current (DC) motor equations and a proportional-integral (PI) current loop controller with cascaded delay and scaling. This completes the plant model for a single axis of motion.

In the Simulink simulation used to generate results later, a quaternion representation, as in Robinson (1958) and Mitchell & Rogers (1968), is used to model the three-dimensional dynamics of the overall system. However, for control design purposes, it is reasonable to assume that the azimuth and elevation bodies are independent of one another. Reaction torque and aircraft motions are then modelled as disturbances on the single axis descriptions.

This paper presents an investigation into the use of constrained predictive control for tracking of angle reference signals. Rate control is not considered, as proportional feedback with the addition of a backlash filter is of satisfactory performance. Standard existing angle control is accomplished using a PI loop with anti-windup and a switch for reducing rate demand near bottom dead centre, otherwise known as the 'nadir'.

One disadvantage of classical PI control lies in the fact that there are several saturation characteristics and hard constraints that are not explicitly considered in a PI controller design. When the turret approaches the 'nadir', the elevation angle approaches 90° and azimuth rate demand becomes very large. Predictive control with constraints is very suitable for this application, as the saturation and hard constraints are incorporated into the control algorithm. Additionally, it is possible to predict the trajectory of the target with some accuracy over a short period. This reference signal can be incorporated into model predictive control (MPC) to predict if the nadir is likely to be approached.

Fig. 1 depicts the system block diagram for the azimuth axis. The elevation axis is almost identical, although r is replaced by q and ψ by θ. The various gains and inertia terms are also different for the two axes. A resolver-to-digital-converter, H_{rdc}, is used for measuring gimbal angle and the rate is computed using a filtered digital differentiator, H_{rate}.

The aim is to control ψ using r_{dem} as the input and ψ_{tgt} as the reference signal. Previously, the block marked 'Angle Control' contained PI with anti-windup and a switch for reducing rate demand near the nadir, but is replaced by a predictive controller.

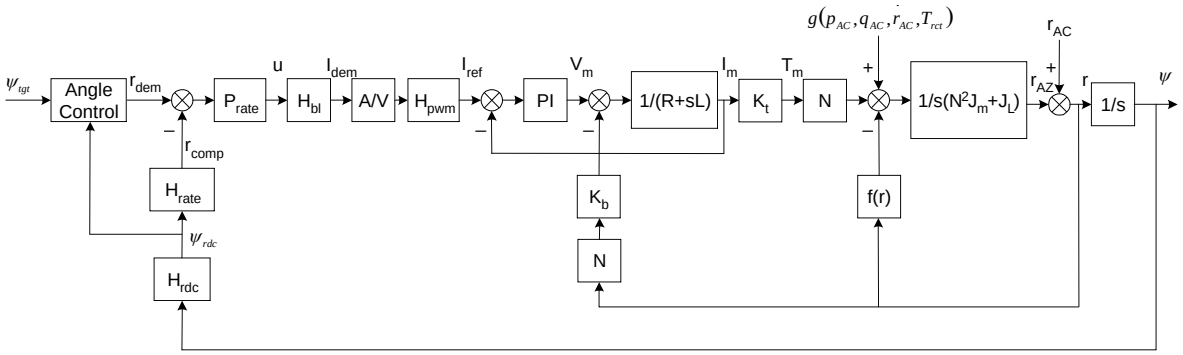

Fig. 1 – System Block Diagram

2. SYSTEM DESCRIPTION

Each axis is described in state-space:

$$\begin{aligned}\mathbf{x}(k+1) &= A\mathbf{x}(k) + Br_{dem}(k) + E\xi(k)\\ \mathbf{y}(k) &= C\mathbf{x}(k)\end{aligned} \tag{1}$$

where

$$\mathbf{x} = \begin{bmatrix} r_{comp} \\ \psi \\ r_{AZ} \\ I_m \\ d \\ V_{mI} \\ I_{ref} \\ I_{dem} \\ u_{k-1} \end{bmatrix}, \mathbf{y} = \begin{bmatrix} \psi \\ I_m \\ V_m \end{bmatrix}, \tag{2}$$

$$\xi = \begin{bmatrix} \xi_1(r_{AC}) \\ \xi_2(p_{AC}, q_{AC}, r_{AC}, f(r), T_{rct}) \end{bmatrix}$$

for the azimuth axis. In order to keep the plant order low, it is assumed that $\psi_{rdc}=\psi$ and the measurement is treated as a state. d is a fictional state intended to represent the constant bristle friction in steady state. It is modelled as a constant that subtracts from the motor torque. V_{mI} is the component of motor voltage, V_m, due to the integral term in the PI current loop. u_{k-1} is a one-step-delayed u signal, which comes from the output of the rate loop proportional gain. It is necessary to delay this term in order to manipulate the plant equations into state space form. The effect of this delay is negligible, however.

The system has three outputs although only angle, ψ, is to be controlled and the other two outputs are constrained as follows:

$$\begin{aligned}|I_m| &< 4.6A = I_{\max}\\ |V_m| &< 150V = V_{\max}\end{aligned} \tag{3}$$

3. KALMAN FILTER

The state vector is only partially measurable, hence it is necessary to estimate the unmeasured states. For this, a Kalman filter is used. Partition the state vector into measured and unmeasured states:

$$\mathbf{x}_m = \begin{bmatrix} r_{comp} & \psi & I_{dem} & u_{k-1} \end{bmatrix}^T \tag{4}$$

$$\mathbf{x}_u = \begin{bmatrix} r_{AZ} & I_m & d & V_{mI} & I_{ref} \end{bmatrix}^T \tag{5}$$

for the azimuth axis. The relevant matrices must then be partitioned:

$$\begin{aligned}\mathbf{x}(k+1) &= A\mathbf{x}(k) + Br_{dem}(k) + E\xi(k)\\ \begin{bmatrix} \mathbf{x}_m(k+1) \\ \mathbf{x}_u(k+1) \end{bmatrix} &= \begin{bmatrix} A_{11} & A_{12} \\ A_{21} & A_{22} \end{bmatrix} \begin{bmatrix} \mathbf{x}_m(k) \\ \mathbf{x}_u(k) \end{bmatrix}\\ &\quad + \begin{bmatrix} B_1 \\ B_2 \end{bmatrix} r_{dem}(k) + \begin{bmatrix} E_1 \\ E_2 \end{bmatrix} \xi(k)\end{aligned} \tag{6}$$

so that:

$$\begin{aligned}\mathbf{x}_u(k) &= A_{22}\mathbf{x}_u(k-1) + \{A_{21}\mathbf{x}_m(k-1)\\ &\quad + B_2 r_{dem}(k-1)\} + E_2\xi(k-1)\end{aligned} \tag{7}$$

$$\begin{aligned}&\{\mathbf{x}_m(k) - A_{11}\mathbf{x}_m(k-1) - B_1 r_{dem}(k-1)\}\\ &= A_{12}\mathbf{x}_u(k-1) + E_1\xi(k-1)\end{aligned}$$

which is in a state-space form. The Kalman filter is then:

$$\begin{aligned}\hat{\mathbf{x}}_u(k-1|k-1) &= \hat{\mathbf{x}}_u(k-1|k-2)\\ &+ L[\{\mathbf{x}_m(k) - A_{11}\mathbf{x}_m(k-1) - B_1 r_{dem}(k-1)\}\\ &- A_{12}\hat{\mathbf{x}}_u(k-1|k-2)]\end{aligned} \tag{8}$$

$$\begin{aligned}\hat{\mathbf{x}}_u(k|k-1) &= A_{22}\hat{\mathbf{x}}_u(k-1|k-1)\\ &+ \{A_{21}\mathbf{x}_m(k-1) + B_2 r_{dem}(k-1)\}\end{aligned}$$

where L is the solution to the Riccati equation.

4. PREDICTIVE CONTROL

Predictive Control is a very powerful controller design technique, as it minimises a quadratic cost function on the system output error and control input, whilst also taking into account constraints on particular signals.

Given a state-space system represented by:

$$\begin{aligned} \mathbf{x}(k+1) &= A\mathbf{x}(k) + B\mathbf{u}(k) \\ \mathbf{y}(k) &= C_y\mathbf{x}(k),\ \mathbf{z}(k) = C_z\mathbf{x}(k) \end{aligned} \tag{9}$$

the aim is to minimise the error between the controlled output, $\hat{\mathbf{z}}(k+i\,|\,k)$, and the reference, $\hat{\mathbf{r}}(k+i\,|\,k)$, whilst restricting the control input change, $\Delta\hat{\mathbf{u}}(k+i\,|\,k)$, over a finite number of steps into the future. If the state is not available for direct measurement, then the measured output, $\mathbf{y}(k)$, is used for state estimation.

The cost function, from Maciejowski (2002), is:

$$\begin{aligned} V(k) &= \sum_{i=H_W}^{H_p} \left\|\hat{\mathbf{z}}(k+i\,|\,k) - \hat{\mathbf{r}}(k+i\,|\,k)\right\|_{Q(i)}^2 \\ &\quad + \sum_{i=0}^{H_u} \left\|\Delta\hat{\mathbf{u}}(k+i\,|\,k)\right\|_{R(i)}^2 \\ &= \left\|Z(k) - T(k)\right\|_Q^2 + \left\|\Delta U(k)\right\|_R^2 \end{aligned} \tag{10}$$

where

$$\begin{aligned} Z(k) &= \begin{bmatrix} \hat{\mathbf{z}}(k+H_w\,|\,k) \\ \vdots \\ \hat{\mathbf{z}}(k+H_p\,|\,k) \end{bmatrix},\ T(k) = \begin{bmatrix} \hat{\mathbf{r}}(k+H_w\,|\,k) \\ \vdots \\ \hat{\mathbf{r}}(k+H_p\,|\,k) \end{bmatrix} \\ \Delta U(k) &= \begin{bmatrix} \Delta\hat{\mathbf{u}}(k\,|\,k) \\ \vdots \\ \Delta\hat{\mathbf{u}}(k+H_u-1\,|\,k) \end{bmatrix} \end{aligned} \tag{11}$$

In order to solve the problem, a prediction of the future controlled outputs, $\hat{\mathbf{z}}(k+i\,|\,k)$, is required. In the simplest case, where the whole state is measured, the expression below is used:

$$\begin{aligned} X(k) &= \begin{bmatrix} \hat{\mathbf{x}}(k+1\,|\,k) \\ \vdots \\ \hat{\mathbf{x}}(k+H_p\,|\,k) \end{bmatrix} \\ &= \begin{bmatrix} A \\ \vdots \\ A^{H_p} \end{bmatrix}\mathbf{x}(k) + \begin{bmatrix} B & & \\ \vdots & & \\ \sum_{i=0}^{H_p-1} A^i B & & \end{bmatrix}\mathbf{u}(k-1) \\ &\quad + \begin{bmatrix} B & \cdots & 0 \\ \vdots & \ddots & \vdots \\ \sum_{i=0}^{H_p-1} A^i B & \cdots & \sum_{i=0}^{H_p-H_u} A^i B \end{bmatrix}\Delta U(k) \end{aligned} \tag{12}$$

and the controlled output estimate formed with:

$$\begin{aligned} \hat{\mathbf{z}}(k+i\,|\,k) &= C_z\hat{\mathbf{x}}(k+i\,|\,k) \\ Z(k) &= \Psi\mathbf{x}(k) + \Upsilon\mathbf{u}(k-1) + \Theta\Delta U(k) \end{aligned} \tag{13}$$

If the tracking error is defined as the difference between the reference vector and the free response of the system:

$$\mathrm{E}(k) = T(k) - \left(\Psi\mathbf{x}(k) + \Upsilon\mathbf{u}(k-1)\right) \tag{14}$$

then $V(k)$ may be restated in terms of the input predictions and tracking error:

$$\begin{aligned} V(k) &= \left\|\Theta\Delta U(k) - \mathrm{E}(k)\right\|_Q^2 + \left\|\Delta U(k)\right\|_R^2 \\ &= \left\| \begin{bmatrix} S_Q\left(\Theta\Delta U(k) - \mathrm{E}(k)\right) \\ S_R\Delta U(k) \end{bmatrix} \right\|^2 \end{aligned} \tag{15}$$

where $Q = S_Q^T S_Q$ and $R = S_R^T S_R$. The aim is to find $\Delta U(k)_{opt}$ to minimise $V(k)$. Ideally, we would have $\begin{bmatrix} S_Q\left(\Theta\Delta U(k) - \mathrm{E}(k)\right) \\ S_R\Delta U(k) \end{bmatrix} = 0$, equivalently stated as $\begin{bmatrix} S_Q\Theta \\ S_R \end{bmatrix}\Delta U(k) = \begin{bmatrix} S_Q\mathrm{E}(k) \\ 0 \end{bmatrix}$. This is a least-squares problem which may be solved for $\Delta U(k)$ at each time step, k, but only $\hat{\mathbf{u}}(k\,|\,k) = \Delta\hat{\mathbf{u}}(k\,|\,k) + \mathbf{u}(k-1)$ is applied.

Constraints are specified in the following form:

$$E\begin{bmatrix} \Delta U(k) \\ 1 \end{bmatrix} \le 0,\ F\begin{bmatrix} U(k) \\ 1 \end{bmatrix} \le 0,\ G\begin{bmatrix} Z(k) \\ 1 \end{bmatrix} \le 0 \tag{16}$$

which may be expressed as a single inequality:

$$\begin{aligned} \begin{bmatrix} F_1 \\ \Gamma\Theta \\ W \end{bmatrix}\Delta U(k) &\le \begin{bmatrix} -F_1 u(k-1) - f \\ -\Gamma\left(\Psi x(k) + \Upsilon u(k-1) - g\right) \\ w \end{bmatrix} \\ \Omega\Delta U(k) &\le \omega \end{aligned} \tag{17}$$

On inspection, the overall problem is of the form:

$$\begin{aligned} &\min_{\Delta U(k)} \left\| \begin{bmatrix} S_Q\left(\Theta\Delta U(k) - \mathrm{E}(k)\right) \\ S_R\Delta U(k) \end{bmatrix} \right\|^2 \\ &= \min_{\Delta U(k)} \begin{Bmatrix} \Delta U(k)^T\left(\Theta^T Q\Theta + R\right)\Delta U(k) \\ -2\Delta U(k)^T\Theta Q\mathrm{E}(k) + \mathrm{E}(k)^T Q\mathrm{E}(k) \end{Bmatrix} \\ &= \min_{\Delta U(k)} \Delta U(k)^T H\Delta U(k) + \Delta U(k)^T G + \mathrm{E}(k)^T Q\mathrm{E}(k) \\ &= \min_{\Delta U(k)} \Delta U(k)^T H\Delta U(k) + G\Delta U(k)^T \end{aligned} \tag{18}$$

subject to $\Omega\Delta U(k) \le \omega$. This is well known as the Quadratic Programming (QP) optimisation problem.

5. TRACKING TURRET EXAMPLE

The azimuth and elevation axes are required to follow realistic reference signals corresponding to target and aircraft movement. For example, if the aircraft rolls in flight, then the target appears to move along an arc of a circular trajectory relative to the turret. Supposing that the turret is at the origin of a coordinate system, a suitable reference may be generated from a circle in three-dimensional space.

Begin by specifying the angle, h, in radians, by which the circle will miss the nadir. If this angle is small, then it will approximately equal the distance of the centre of the circle from the origin. If the trajectory is traced out by a unit vector, then the circle radius is $r = \sqrt{1-h^2}$.

The remaining parameters are rotation rate, ω, initial phase on the circle, ϕ, and azimuth angle of the circle, θ. Coordinates of the unit vector in an (x,y,z) system may be computed by transformation. Fig. 2 shows an example when $h=1°=0.0175rad$ and $\theta=45°$.

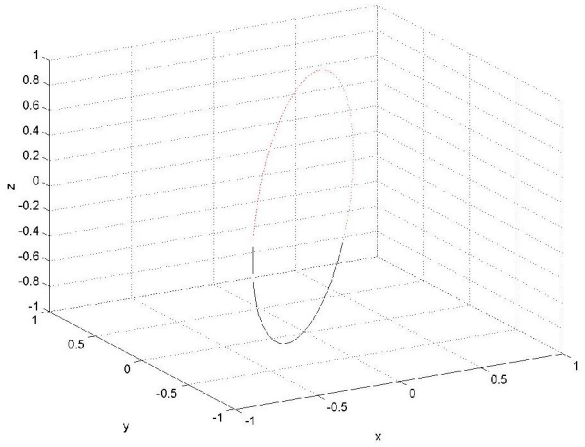

Fig. 2 – Reference Vector Trajectory

The circle is at 45° to the y-z plane in accordance with θ, and the origin is approximately 0.0175 from the centre of the circle, in agreement with h.

The example vector in (x,y,z) is then translated into demands on the azimuth and elevation of the turret. The azimuth reference is $tan^{-1}(y/x)$ and the elevation reference is $sin^{-1}(z/1)$. Three points on the circle may be used to extrapolate the azimuth and elevation demands into the future, as depicted in Fig. 3, corresponding to the darkened arc (Fig. 2).

The reference demand extends 1.5 seconds into the future and $\omega=60°/s$, ϕ=150°. Fig. 4 depicts the rate demand in the example, where azimuth rate peaks at $60rad/s$ when the elevation angle is $-89°$. This illustrates the nadir phenomenon well. If h shrinks to less than $1°$, the azimuth rate demand peak will grow, until it becomes infinite when h is zero. However, due to the motor voltage and current constraints in equation (3), the maximum acceleration and velocity of each axis are also constrained. In the azimuth case, these maxima are $80rad/s^2$ and $6.08rad/s$ respectively. The predictive controller can cope with the huge rate demand via the use of future knowledge and constraint handling.

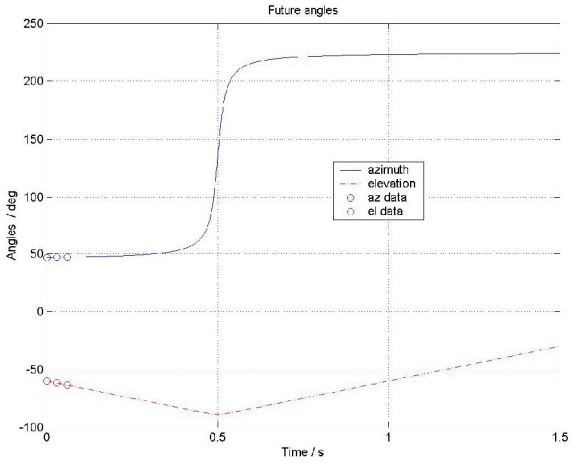

Fig. 3 – Angle Reference Trajectory

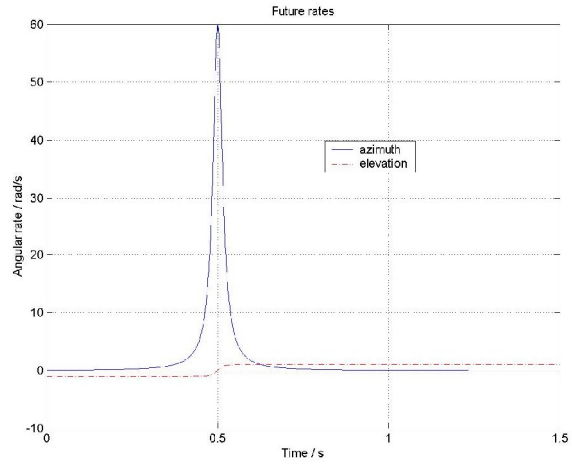

Fig. 4 – Rate Reference Trajectory

In the control example that follows, the above angle reference will be applied to both the MPC controller and the standard PI controller.

The sample time must be short in order to accurately estimate the rapid response of current and voltage in the motor controller. 1ms is selected, as this is the maximum capability of the Selex hardware. The output prediction horizon is 150 steps or 0.15 seconds and the input horizon is 10 steps or 0.01 seconds for both azimuth and elevation axes. These are the maximum horizon sizes without introducing ill-conditioned matrices and numerical errors. The error weightings are $Q(i)=1+0.075i$ for azimuth and $Q(i)=1+0.15i$ for elevation. The input weightings are $R(i)=0.4-0.02i$ in both cases. The increasing output weights and decreasing input weights improve the overshoot and settling characteristics, since the controller gain is effectively increased as the setpoint is approached. The time constant for the exponential trajectory from present output to reference trajectory is 0.1 seconds in both cases.

Figs. 5 and 6 give a comparison between the existing PI controller and the MPC controller when the above example reference signal is applied.

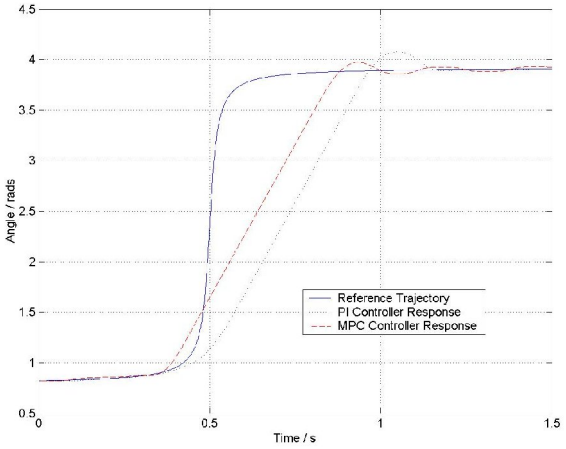

Fig. 5 – Azimuth Angle

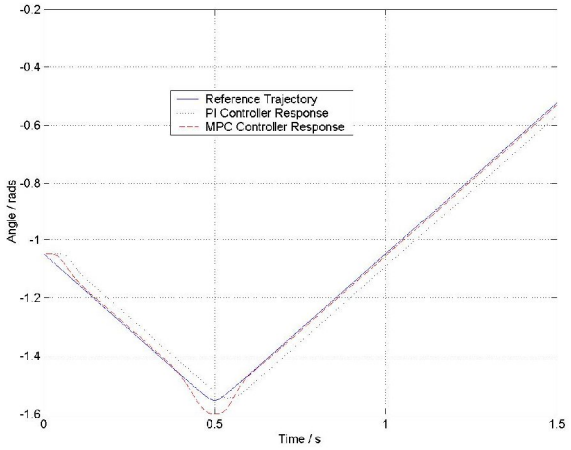

Fig. 6 – Elevation Angle

Fig. 5 clearly shows that MPC anticipates the nadir and begins azimuth rotation earlier. Overshoot is also smaller, although the PI plot settles whilst the MPC plot exhibits small limit cycles due to the friction model and estimates. Fig. 6 demonstrates superior performance by MPC for the elevation angle, where the offset is negligible compared to the PI case. At the nadir after 0.5 seconds, the MPC plot does overshoot, but this is again due to friction, which is now discussed in terms of state estimates.

The r_{AZ} and I_{ref} estimates are very accurate and not shown here. Figs. 7 to 9 show the state estimates of azimuth axis motor current, disturbance and motor voltage, V_{mI}, due to the PWM integrator.

The flip in sign of the disturbance is responsible for the poor current and voltage estimates and the limit cycle seen in Fig. 5. A similar effect is seen at the lowest point of elevation, where the elevation disturbance flips in sign and degrades the other state estimates.

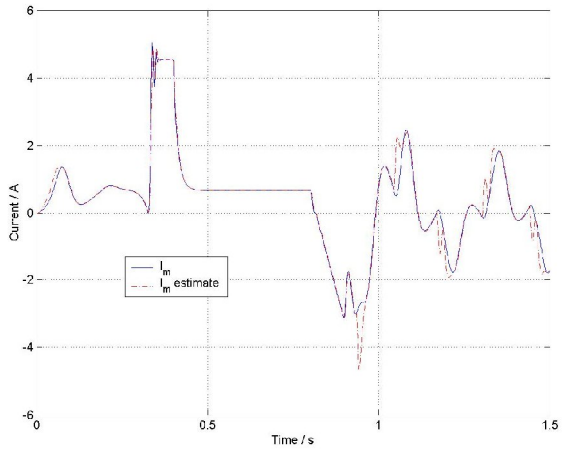

Fig. 7 – Azimuth Current

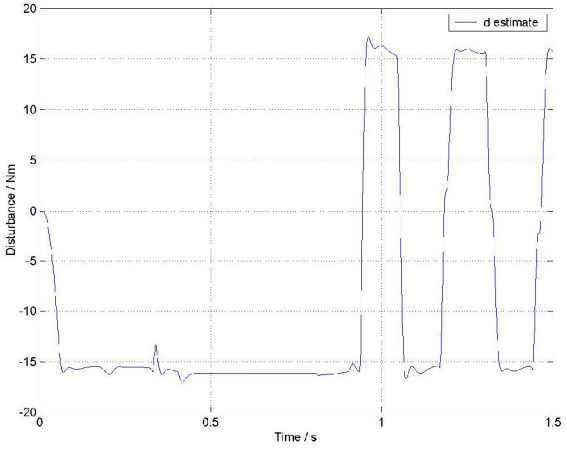

Fig. 8 – Azimuth Disturbance

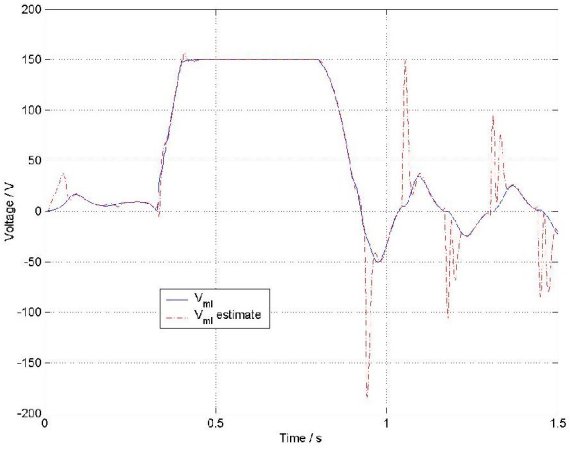

Fig. 9 – Azimuth Voltage from PWM Integrator

Note that the constraint in inequality (3) is obeyed for the motor current and is also obeyed for motor voltage, but this cannot be seen directly from Fig. 9. Also, the results are not greatly affected by plant-model mismatch, as the Kalman filter tends to express the unmodelled behaviour in terms of the *d* state. There is not sufficient space in this paper to illustrate this fact, however.

6. CONCLUSIONS

A novel application of constrained model predictive control to a servo-driven tracking turret simulation has been demonstrated. The turret is modelled in state-space, where four of the states are measurable and five are estimated using a Kalman filter. It is demonstrated that around the nadir point, where the system is driven to saturation limits and will potentially lose a target, performance of MPC is superior to that of the existing classical PI controller.

The existence of a reliable reference signal, extrapolated from the target trajectory, allows MPC to anticipate the large rate demand near to the nadir. This gives a much earlier response, which is vital for target acquisition and following in this high bandwidth tracking application. The system constraints encapsulated in MPC also produce less overshoot of the azimuth angle and would do so for the elevation angle, given better friction estimates.

The main problem with the MPC is that friction in the turret is not well modelled in state-space, which tends to produce poor state estimates when friction effects are particularly active. The friction is modelled as a constant with slight excitation by white noise, which is acceptable when turret angles are increasing or decreasing monotonically. However, when the rate changes sign, the flip in friction sign tends to give small limit cycles. As further work, it may be possible to revise the state-space friction model so that better-behaved estimates are obtained. Indeed, the underlying non-linear model in the simulation may need revision, as it is unclear how accurately the real friction of the turret is represented.

Another problem with the MPC is that the 1ms sample time, dictated by estimating the high bandwidth motor controller, prevents use of prediction horizons beyond 0.15s due to numerical errors. This application would benefit from accurately predicted target trajectories further into the future, so extended horizons are desirable. There is not much scope to reduce the sample rate, due to potential aliasing in the estimator, but more numerically robust QP solvers could be investigated.

Finally, the MPC controller should be tested with real hardware, but software limitations in implementing the QP solver have so far prevented this.

ACKNOWLEDGEMENTS

The authors are grateful to Selex Sensors & Airborne Systems for their general support, and wish to offer thanks for the mathematical turret model and Simulink simulation on which the study was based. Thanks also to the EPSRC for funding this work on Grant GR/S60396/01. The first author would like to thank Dr. Nick Brignall and Matt MacDonald at Selex for their invaluable contribution to this work. Also thanks to Prof. Mike Grimble, Dr. Reza Katebi and the University of Strathclyde Industrial Control Centre for esteemed advice and support.

REFERENCES

Maciejowski, J.M. (2002). *Predictive control with constraints*. Prentice-Hall, Pearson Education Limited, Harlow, England.

Masten, M.K. (1996). Electromechanical systems for optical target tracking systems. In: *Selected Papers on Precision Stabilization and Tracking Systems for Acquisition, Pointing, and Control Applications* (Masten, M.K, Stockum, L.A (Ed)), SPIE Milestone Series, Volume MS 123.

Mitchell, E.E.L., and A.E. Rogers (1968). Quaternion parameters in the simulation of a spinning rigid body. In: *Simulation: The Dynamic Modeling of Ideas and Systems with Computers* (John McLeod, P.E. (Ed)).

Robinson, A.C. (1958). On the use of quaternions in simulation of rigid-body motion, *Wright Air Development Center (WADC) Technical Report 58-17*.